Seasonal variability of natural water chemistry affects the fate and behaviour of silver nanoparticles

Ellis, Laura-Jayne; Baalousha, Mohammed; Valsami-Jones, Eugenia; Lead, Jamie

DOI:
10.1016/j.chemosphere.2017.10.006

Document Version
Publisher's PDF, also known as Version of record

Citation for published version (Harvard):
Ellis, L-JA, Baalousha, M, Valsami-Jones, E & Lead, JR 2018, 'Seasonal variability of natural water chemistry affects the fate and behaviour of silver nanoparticles', Chemosphere, vol. 191, pp. 616-625. https://doi.org/10.1016/j.chemosphere.2017.10.006

Chemosphere 191 (2018) 616–625

Contents lists available at ScienceDirect

Chemosphere

journal homepage: www.elsevier.com/locate/chemosphere

Seasonal variability of natural water chemistry affects the fate and behaviour of silver nanoparticles

Laura-Jayne A. Ellis [a], Mohammed Baalousha [b, *], Eugenia Valsami-Jones [a], Jamie R. Lead [a, b, **]

[a] School of Geography, Earth and Environmental Sciences, University of Birmingham, Edgbaston, Birmingham, B15 2TT, UK
[b] Center for Environmental Nanoscience and Risk (CENR), Department of Environmental Health Sciences, Arnold School of Public Health, University of South Carolina, Columbia, 29208, USA

HIGHLIGHTS

- Aquatic microcosms were used to study AgNPs transport and behaviour in seasonal variations of natural water.
- NP stability was influenced by the seasonal variations in chemistry of the natural water and NP coating.
- A diffusion-sedimentation model was used to calculate AgNP migration behaviour in natural waters.

GRAPHICAL ABSTRACT

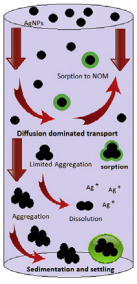

ARTICLE INFO

Article history:
Received 9 June 2017
Received in revised form
19 September 2017
Accepted 1 October 2017
Available online 23 October 2017

Handling Editor: Petra Petra Krystek

Keywords:
PVP and citrate coated silver nanoparticle (AgNPs) transformations
Aggregation
Natural water
Diffusion
Sedimentation
Fate and behaviour

ABSTRACT

Understanding the environmental behaviour of nanoparticles (NPs) after release into aquatic systems is essential to predict the environmental implications of nanotechnology. Silver nanoparticles (AgNPs) represent a major class of engineered NPs with a significant potential for environmental impact. Therefore, investigating their transformations in natural waters will help predict their long term environmental fate and behaviour. AgNPs were characterized in natural lake water collected seasonally from the same freshwater source, using column microcosms to assess their behaviour and transport at different depths. Building on our previous work using similar systems with synthetic waters, the influence of water chemistry and NP surface modifications on colloidal stability and dissolution in natural lake water over time was investigated. A simple sedimentation-diffusion model parameterized by the particle properties and total Ag concentration was successfully used to understand AgNPs transport behaviour. PVP coated AgNPs remained colloidally stable, with their transport in the water column dominated by diffusion, and exhibited no significant or substantial changes in data or model parameters for different seasons. Citrate coated AgNPs were susceptible to rapid aggregation, sedimentation, dissolution and reprecipitation; their transport in the water column was determined by both diffusion and sedimentation.

* Corresponding author.
** Corresponding author. Center for Environmental Nanoscience and Risk (CENR), Department of Environmental Health Sciences, Arnold School of Public Health, University of South Carolina, Columbia, 29208, USA.
E-mail addresses: Mbaalous@mailbox.sc.edu (M. Baalousha), JLead@mailbox.sc.edu (J.R. Lead).

https://doi.org/10.1016/j.chemosphere.2017.10.006

1. Introduction

Silver nanoparticles (AgNPs) represent a major class of engineered NPs with significant potential for environmental impact (Lodeiro et al., 2016; Fabrega et al., 2011a, 2011b). The estimated production of nano-enabled products has risen from less than 10 tons per year in 2011 (Hendren et al., 2011) to 300 tons per year in 2015 (King et al., 2015). Releases of AgNPs from consumer products including textiles (Benn and Westerhoff, 2008) and personal health care products (Nowack et al., 2012), have led to wide environmental dispersal and increased concentrations (Huynh and Chen, 2011; Baalousha et al., 2013; Mueller and Nowack, 2008). Environmental AgNP concentrations are estimated at 30.1 mg kg^{-1} in sediments, 2.3 mg kg^{-1} in sludge and treated soils, and 2.2 μg L^{-1} in surface waters (Sun et al., 2016). Increased AgNP concentrations likely pose significant hazards to marine life, particularity as toxic effects have been identified in the μg L^{-1} concentration range (Fabrega et al., 2011b; Asghari et al., 2012).

The environmental fate of AgNPs will be influenced by water chemistry, biology and the NP physicochemical properties. Sedimentation can reduce AgNP migration (Bae et al., 2013) although interactions with natural organic macromolecules (NOM) can increase persistence in aquatic systems (Chen and Elimelech, 2007; Lowry et al., 2012). Furthermore, the nature of the NP surface stabilizer will likely impact NP transformations and subsequent fate and behaviour (Ju-Nam and Lead, 2008; Chinnapongse et al., 2011; Hitchman et al., 2013; Baalousha et al., 2015). Charge stabilized AgNPs mostly aggregate in high ionic strength waters, irrespective of NOM concentrations, due to charge neutralization, shielding and bridging mechanisms interactions (Chen and Elimelech, 2007; Baalousha et al., 2013). However, at low ionic strength, high NOM concentrations can reduce aggregation (Chinnapongse et al., 2011). Sterically-stabilized AgNPs are generally more colloidally stable, less affected by solution chemistry and less likely to dissolve or aggregate (Hitchman et al., 2013; Sharma et al., 2014).

Understanding the impacts of AgNPs release into natural water is essential to predict potential exposures and environmental and human health and safety implications (Kennedy et al., 2010; Gottschalk et al., 2013; Pokhrel et al., 2014; Nowack et al., 2015). Building on our previous work with synthetic media (Ellis et al., 2016), the objective of this study is to investigate the effects of seasonally changing natural lake water on differently capped AgNPs, using column microcosms to identify fate, behaviour and transformations at different water depths. To our knowledge, different depth water analysis (surface, middle and bottom) over four different seasonal time points of natural water, with the use of a simple sedimentation-diffusion model has not yet been explored in the literature.

2. Experimental materials and methods

Details of the experimental set-up is given in our previous work (Ellis et al., 2016). Here we use natural lake water collected at different seasons instead of synthetic waters used in the previous study.

2.1. Materials

All chemicals were commercially available from Sigma Aldrich (Dorset, UK) of analytical reagent grade. Ultra-pure water (UPW) (resistivity 18.2 MΩ cm) was used throughout the experiments. Natural water, described in Section 2.5, was collected from the Vale Lake at the University of Birmingham campus, UK (Table 1, Figure SI.1 and Table SI.1).

2.2. Nanoparticle synthesis and purification

Citrate and PVP coated AgNP synthesis protocols are described in detail elsewhere (Cumberland and Lead, 2009; Tejamaya et al., 2012). Briefly, all AgNPs were synthesized under ambient

Table 1
Summary of key observations of AgNP behaviour.

Season/water type from the Vale Lake	TOC (mg L^{-1})	pH	PVP nanoparticle diameter calculated using the model (nm)	Citrate nanoparticle diameter calculated using the model (nm)	Observation of 2nd UV −vis peak (nm) for the citrate AgNPs	Overall observations and conclusions
Spring	13	7.5	17.3	10	none	**PVP and citrate coated:** no aggregation, little evidence of dissolution. Diffusion dominated transport
Summer	32	7.6	10	10	500	**PVP coated:** no aggregation, little evidence of dissolution. Diffusion dominated transport. **Citrate coated:** More complex behaviours; high NOM concentration, evidence for dissolution and reprecipitation. Since the model does not suggest size increases/decreases, two conclusions maybe drawn based on UV and metal concentration data 1) No aggregation and losses are due to sorption to NOM 2) Metal concentration data suggests Ag losses, which could be consistent with limited aggregation/ sedimentation supported by the model calculated AgNP size.
Autumn	28	7.4	10	88.4	530	**PVP coated:** no aggregation, little evidence of dissolution. Diffusion dominated transport **Citrate coated:** Aggregation, increased modelled size, increased sedimentation velocity (U), some evidence of dissolution, high NOM concentration: possibly fibrillar type consistent with aggregation.
Winter	4	7.2	13.7	226.1	600	**PVP coated:** no aggregation, little evidence of dissolution. Diffusion dominated transport **Citrate coated:** Evidence of aggregation, much larger modelled size, low NOM concentration, little/ no dissolution, increased sedimentation velocity.

atmospheric conditions (i.e in air). Citrate-AgNPs were prepared using a 0.25 mM silver nitrate ($AgNO_3$) solution mixed with a 0.25 mM sodium citrate solution, followed by the addition of 0.25 mM sodium borohydride ($NaBH_4$). The solution was heated at 100 °C for 2 h, whilst stirring vigorously. Suspensions of PVP-AgNPs (Tejamaya et al., 2012) were prepared in an ice-cold solution of (2 mM) $NaBH_4$ and PVP (M_w 10,000, Sigma Aldrich). The addition of $AgNO_3$ (1 mM) was titrated at 1 drop per second under vigorous stirring. Ultrafiltration was used to remove excess dissolved Ag and citrate/PVP, using a 1 kDa cellulose membrane in a 350 mL Millipore stirred cell ultrafiltration system under nitrogen gas (N_2). Details of the ultrafiltration procedure is reported elsewhere (Cumberland and Lead, 2009). Suspensions of AgNPs were refrigerated at 4 °C until use. Further information is provided in the supporting information (Section SI.1.2, Figures SI.2- SI.7: Tables SI.2 and SI.3).

2.3. Microcosm experiments

The design of the microcosms is described in detail elsewhere (Ellis et al., 2016). Briefly, the microcosms were tall (100 × 25 cm) cylindrical columns with a liquid capacity of 43 L. In all experiments, the exterior walls were shielded from all light sources to simplify understanding of transformations by preventing photochemical transformations of AgNPs. AgNPs were introduced through a mesh at a depth of 5 cm below the surface (Section SI.1.3: Figure SI.8). Assuming a uniform distribution of Ag throughout the water column, the mass of AgNPs (4.3 mg Ag) added to the columns was estimated to give a final uniform concentration of 100 μg Ag L^{-1}, assuming diffusive transport only, with no sorptive or other losses. The concentration was selected to be close as possible to predicted environmental concentrations of AgNPs (Gottschalk et al., 2013), while maintaining sufficient particle concentration to enable analysis, limited by UV–visible spectrometry (UV–vis).

2.4. Characterisation of AgNPs

A multi-method analytical approach was applied to identify the migration and physicochemical transformations in each of the seasonal variants of the natural lake water. Dynamic light scattering (DLS) was used to measure the 'as prepared' AgNPs hydrodynamic size using a Malvern Nanosizer 5000. Due to interference issues from natural water colloids, DLS was not suitable for the main microcosm experiments (Piccapietra et al., 2011). Atomic force microscopy (AFM) analysis for the 'as prepared' AgNPs was performed using an XE-100 AFM (Park systems Corp). A JEOL 1200EX 100kv LaB6 Max system and a Tecnai F20 Field Emission gun (FEG) transmission electron microscopy (TEM) coupled with an energy dispersive X-ray spectrometry (EDS) detector from Oxford Instruments, were used to perform particle core size analysis and EDS. Samples were adhered to a carbon coated copper grids (Agar Scientific). Images were analyzed using Digital Micrograph software (Gatan Inc, USA).

A Jenway 6800 double beam UV–visible spectrometer (UV–vis) was used to measure the surface plasmon resonance (SPR) of the 'as prepared' AgNPs suspensions, and samples were withdrawn from the microcosms using a 10 cm long path length cuvette (Ellis et al., 2016). Flame atomic absorption spectrometry (FAAS, Perkin Elmer instrument AAnalyst 300), with an air-acetylene mixture was used to measure total silver (Ag) concentrations. Ultrafiltration combined with FAAS also enabled the estimation of the percentage of dissolved Ag and AgNPs concentrations in each of the samples taken from the surface and bottom sampling depths. This information was used to indicate the dissolution and reprecipitation of the AgNPs over time.

2.5. Water preparation and sampling

Natural water samples were collected from the Vale Lake located the University of Birmingham campus, UK (Figure SI.1, Table SI.1, Table 1) at four different time points, representing winter (January) spring (April), summer (July) and autumn (October) in the UK. All water samples were collected around 12 noon, and had near-neutral pH (Table 1). The concentration of total organic carbon (TOC) in the natural lake water can be used as an indicator of the total NOM concentration including; biopolymers, produced as biological waste by bacteria and algae, humic substances; including humic acids (HA), fulvic acids (FA), fibrillar polysaccharides (Hendricks, 2006; Diegoli et al., 2008) and all other dissolved organic carbon. Water from just below the lake water surface was collected in acid washed heavy duty plastic containers (15 L) (Doucet et al., 2004). Transportation time was approximately 10–15 min between water collection and returning to the laboratory. The water was filtered through muslin cloth to remove large debris and left for 24 h prior to use, to allow smaller particles to settle. Chemical analysis of the natural water for a suite of major ions was performed using an Agilent 7500ce inductively coupled plasma–mass spectrometry (ICP-MS) with a collision cell. TOC concentrations were measured using a Shimadzu TOC-V CSH instrument. The characteristics of the natural water for each season are presented in Table SI.1.

Water sampling from the microcosms is described elsewhere (Ellis et al., 2016). Briefly, 5 mL samples were withdrawn from the surface introduction point, middle (50 cm from the surface and bottom) and bottom (90 cm from the surface) of the microcosm column, using six inch stainless steel hypodermic syringes. Sampling was conducted at time 0, 0.5, 1.5, 3.5, 5.5 and 8 h on day 1, then daily for the first 14 days, and once again on days 21 and 28, respectively. Additionally, samples from the surface and bottom were analyzed between days 1–14, 21 and 28, to assess the dissolved and particulate concentration (% Ag) using ultrafiltration (Doucet et al., 2004). The microcosm experiments were conducted in static columns with no artificial mixing and at room temperature (20 ± 2 °C).

2.6. Modelling the transport of Ag concentrations

Determining the migration behaviour of the AgNPs is particularly important for establishing their fate in natural water systems. The migration behaviour of the AgNPs in each of the seasonal variations of natural lake water was determined using the total Ag concentration profiles from samples measured the surface, middle and bottom locations of the microcosm column. The model is presented elsewhere (Ellis et al., 2016) and is briefly described below. Diffusion and sedimentation transport processes can be modeled by the diffusion-sedimentation equation to calculate the Ag concentration profile as a function of time for each sampling point in the water column (Eq. (1)) (Socolofsky and Jirka, 2005). A summary of all units and constant values are provided in Table SI.4.

$$\frac{\partial C}{\partial t} + \frac{\partial \mu_i C}{\partial x_i} = D\frac{\partial^2 C}{\partial x_i^2} \quad (1)$$

The boundary conditions that satisfy the experimental conditions for Eq. (1) are: i) absence of AgNPs in the water column at $t = 0$; that is $C_{Ag} = 0$ at $t = 0$ for $0 < x < L$, ii) introduction of AgNPs at the top of the water column; that is $C_{Ag} = C_0$ at $t = 0$ and $x = 0$, and iii) no flux at the bottom of the column; that is $dC/dx = 0$, at $x = L$. Using these boundary conditions, the analytical solution of Eq. (1) can be given by Eq. (2):

$$C(x,t) = \frac{M_{Ag}}{A\sqrt{4\pi Dt}}\left(\exp\left(-\frac{(x-x_0)^2}{4Dt}\right) + \exp\left(\frac{(x-x_i)^2}{4Dt}\right)\right) \quad (2)$$

This analytical solution accounts only for AgNP diffusion and sedimentation and does not account for AgNP dissolution, sorption or accumulation at the bottom of the microcosm following sedimentation/settling. Discrepancies between the measured and modeled Ag concentrations can be explained partially by dissolution and sorptive losses. The NP diffusion coefficient (D) and sedimentation velocity (U) can be described by Stokes-Einstein Law for the diffusion in solution (Eq. (3)) and Stokes equation (Eq. (4)) (Hinderliter et al., 2010):

$$D = \frac{KT}{3\pi\mu\, d} \quad (3)$$

$$U = \frac{g\left(\rho_\rho - \rho_f\right)d^2}{18\mu} \quad (4)$$

The fitting parameters (AgNP diameter and mass of Ag introduced to the water column) were optimized by Solver software in Microsoft Excel by minimizing the weighted square error calculated using Eq. (5):

$$X^2 = \sum \frac{(O-E)^2}{\sigma^2} \quad (5)$$

where σ^2 is the variance of the measured Ag concentrations, O is the observed concentration data, and E is the expected Ag concentration data. The measured Ag concentrations at the middle sampling point were used in the fitting process, as these concentrations are likely to be most accurate concentrations. Table 2 describes the model outputs, which were optimized by the solver software for each water condition and particle type. The model therefore explicitly accounts for NP diffusion and sedimentation behaviour, but does not account for dissolution explicitly. Dissolution can therefore be used as an explanation in case of less than optimal model fits.

Table 2
Silver mass, diameter, diffusion coefficient and settling velocity calculated by fitting the measured concentration using the diffusion-sedimentation equation. M_{Ag} mass of Ag introduced to the water column (mg). D diffusion coefficient, U settling velocity, d diameter (nm). The fitting parameters (nanoparticle diameter and mass of Ag introduced to the water column) were optimized by Solver software in Microsoft Excel by minimizing the weighted square error.

Model Parameters				
Season	M_{Ag} (mg)	d (nm)	D (10^{-12} m^2 s^{-1})	U (10^{-8} m s^{-1})
PVP AgNPs				
Spring	3.7	17.3	24.8	0.15
Summer	2.4	10	43	0.05
Autumn	2.9	10	43	0.05
Winter	2.3	13.7	31.4	0.09
Cit AgNPs				
Spring	4.1	10	43	0.05
Summer	1.6	10	43	0.05
Autumn	2.0	88.4	4.9	4
Winter	2.0	226.1	1.9	26

3. Results and discussion

3.1. AgNP characterisation

The physicochemical properties of the pristine AgNPs are summarized in the supporting information section (Table SI.2 and Table SI.3). Citrate-AgNPs were spherical particles (Figure SI.4) with an average core size of 11 ± 3 nm (TEM) and PVP-AgNPs were comparable (Figure SI.7) at 11 ± 2 nm (TEM). The SPR was measured at 393 nm for the citrate-AgNPs (Figure SI.2) and 401 nm for the PVP-AgNPs (Figure SI.5), consistent with previously reported data (Tejamaya et al., 2012).

3.2. Migration behaviour of AgNPs in lake water

3.2.1. PVP-AgNPs

Fig. 1 shows, for each season (spring, summer, autumn and winter), the behaviour of the PVP coated AgNPs in microcosms at each depth. For all conditions, no major changes in the Ag concentration were observed for the PVP-AgNPs in any of the microcosms, regardless of the composition of the water due to seasonality (spring, summer, autumn or winter). For each season, the low concentrations of Ag over the first 24 h in the middle (Fig. 1B, E, 1H and 1K) and bottom sampling points of the columns (Fig. 1C, F, 1I and 1L), suggests particle dispersion was a relatively slow process between introduction and sampling. Collectively, after 7 days, the average maximum total Ag concentration measured at each depth in all four seasonal water conditions was 65 ± 10 μg L^{-1}. This uniform concentration between each depth (and per season) remained consistent for the duration of the study, following a pattern commonly associated with diffusion controlled transport. Therefore, it is suggested that PVP-AgNP behaviour is the same throughout the microcosm columns, where losses of Ag are reflected in the mass of the introduced AgNPs (M_{Ag}) (Table 2), sorptive losses to the interior surfaces of the microcosm walls and, at later times, and sample removal from the system (30 mL per day).

The modelled total Ag concentration was established using Eq. (2) and statistically optimized by minimizing the weighted sum of squared fitting errors (Eq. (5)) to produce the best fits between the two sets of data (experimental and modelled in Fig. 1). The statistical fitting produced the average particle diameter, M_{Ag}, diffusion coefficient (m^2 s^{-1}), sedimentation velocity (m s^{-1}) (Table 2), and the predicted total Ag concentration over time (Fig. 1) using the model units and parameters listed in Table SI.4. The modelled sizes of the PVP-AgNPs were 17.3 nm (spring), 10 nm (summer and autumn), 13.7 nm (winter) (Table 2). The estimated sizes from the model were comparable to the 'as prepared' PVP-AgNPs (Table SI.3), further suggesting limited aggregation. For all conditions, the values for the diffusion coefficient and the sedimentation velocity were inversely proportional for each water condition (Table 2). Therefore, for the size range considered in this paper, as the AgNP size gradually decreases, the values for diffusion coefficient gradually increase and thus the sedimentation velocity decreases.

To complement the total Ag concentration data, ultrafiltration was used to estimate the proportion of dissolved Ag at the surface and bottom (Table SI.5). In most cases, higher AgNP concentrations and lower dissolved Ag silver concentrations were measured per season compared to the citrate-AgNPs, further indicating limited dissolution of PVP-AgNPs. On day 28, the PVP-AgNPs represented on average 75% of the total Ag at the top and bottom of the columns.

To improve our understanding of the NP metal concentration data, additional characterisation of the PVP-AgNPs was conducted including UV–vis and TEM. Changes in AgNPs properties can be identified via changes in their SPR (Chinnapongse et al., 2011). In most cases, the UV–vis profiles presented in Fig. 2 show a single

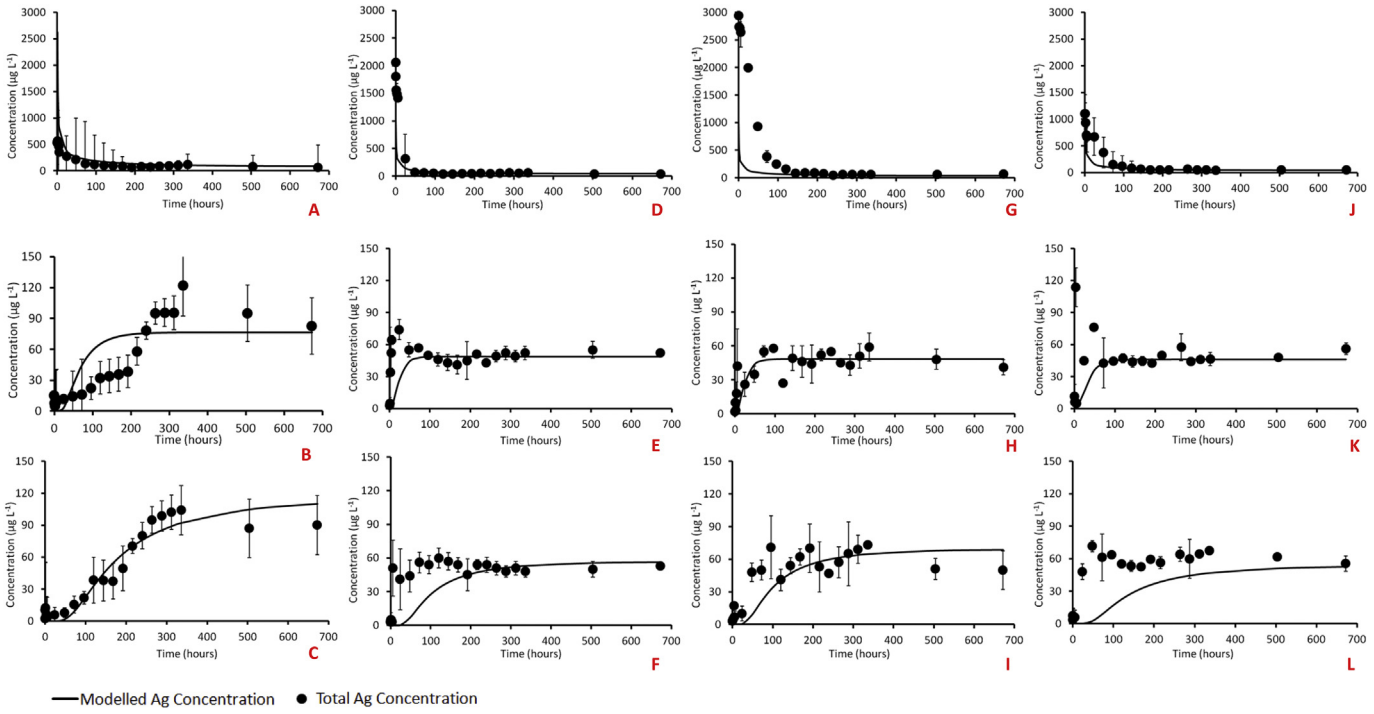

Fig. 1. Observed and modelled total Ag concentrations over time for the PVP-AgNPs study in the surface, middle and bottom depths of the microcosm, in each of the water conditions: A) spring: surface water, B) spring: middle depth water, C) spring: bottom depth water, D) summer: surface water, E) summer: middle depth water, F) summer: bottom depth water, G) autumn: surface water, H) autumn: middle depth water, I) autumn: bottom depth water, J) winter: surface water, K) winter: middle depth water and L) winter: bottom depth water. Dots show the average concentrations of three independent triplicates, error bars represent the standard deviation of the measured concentrations in the three replicated and the solid lines is the fitted model. Mass of AgNPs introduced to the column fixed at 4.3 mg.

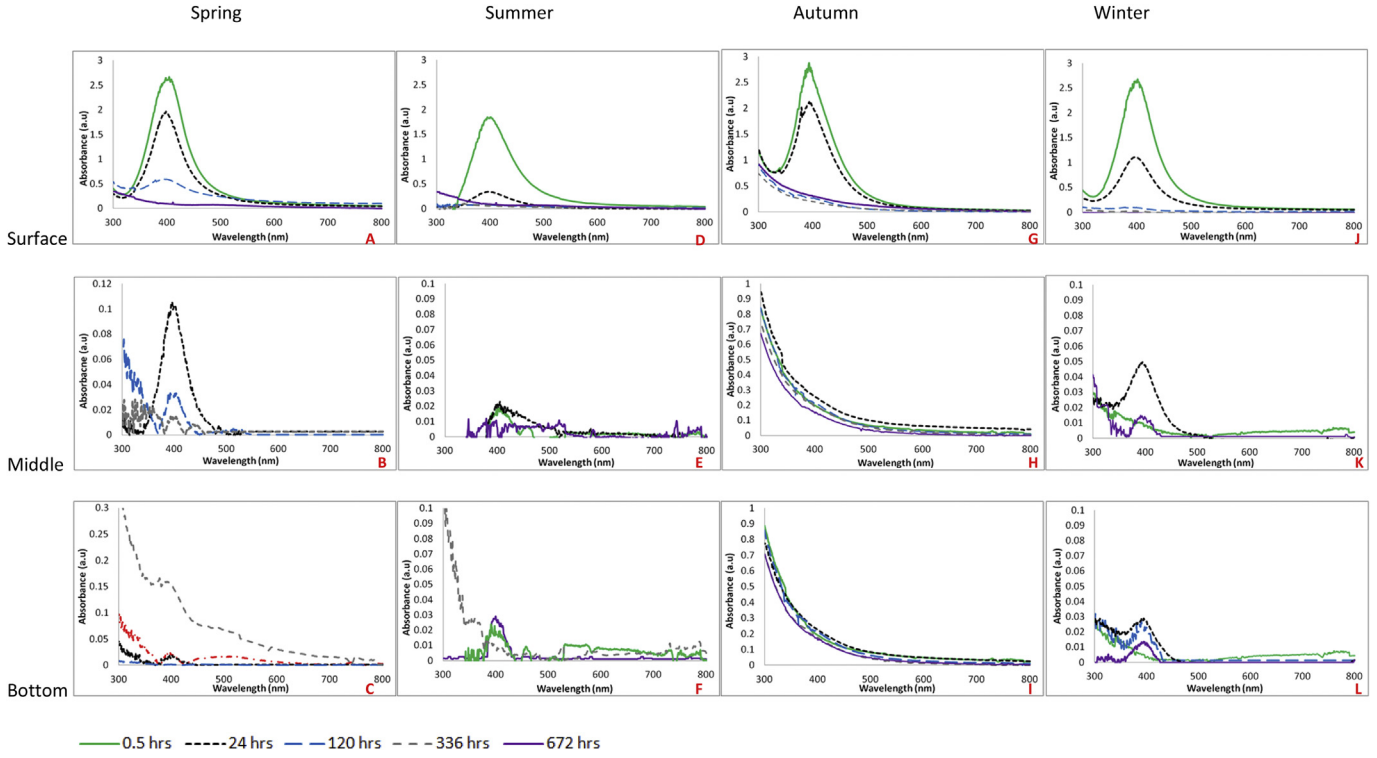

Fig. 2. Comparison SPR profiles of PVP-AgNPs over time for the surface, middle and bottom depths of the microcosm, in each of the water conditions, A) spring: surface water, B) spring: middle depth water, C) spring: bottom depth water, D) summer: surface water, E) summer: middle depth water, F) summer: bottom depth water, G) autumn: surface water, H) autumn: middle depth water, I) autumn: bottom depth water, J) winter: surface water, K) winter: middle depth water and L) winter: bottom depth water.

peak centered at 400 nm, similar to SPR value for the as synthesized PVP-AgNPs and to SPR values reported in the literature for small spherical PVP-AgNPs (Tejamaya et al., 2012; Roh et al., 2013). Furthermore, AgNP concentration and migration between each depth can be traced by identifying the differences in the UV–vis absorbance at the SPR wavelength (λ_{max}) over time in each depth. For example, Fig. 2A shows the UV–vis absorbance profile for PVP-AgNPs at the microcosm surface in the spring seasonal water. Absorbance at λ_{max} decreased from of 2.6 (a.u) at 0.5 h (green line) to 1.7 (a.u) at 24 h (dashed black line). Comparing the same time points at the middle depth (Fig. 2B), the absorbance at λ_{max} at 0.5 h (not displayed in the graph for clarity) is 0.007 (a.u), suggesting that the PVP-AgNPs have not yet migrated to this depth. At 24 h, the absorbance at λ_{max} is higher at 0.11 (a.u), indicating the migration of PVP-AgNPs into the lower depths.

The SPR for PVP-AgNPs was detectable at each sampling depth for the duration of the study (672 h/28 days inclusive) in each of the natural water conditions. The absorbance at 300 nm in each spectrum was due to interferences of the NOM producing band tailing; NOM has a an SPR at approximately 254 nm (Fig. 2H and J) (Hendricks, 2006; EPA, 2009).

TEM samples were collected at 24 h and 72 h post release (Fig. 3, Figures SI.9, SI.11-SI.13 and Table SI.6), which identified morphologically small spherical AgNPs, comparable to sizes produced by the model and those of the 'as prepared' PVP-AgNPs. This information supports the model and the UV–vis data, providing additional evidence that PVP-AgNPs remain colloidally stable in each seasonal variation of the natural water and migrate through the microcosms via diffusion. The stability of the PVP-AgNPs is due to the structural complexity of PVP polymer forming a thick surface coating layer strongly bound to the surface of the AgNPs (Kvitek et al., 2008). PVP is strongly bound to AgNPs and stabilizes AgNPs via steric mechanisms. Therefore, the polymer coatings are largely not sensitive to presence of high ionic strengths (Ju-Nam and Lead, 2008; Afshinnia et al., 2017). The role of adsorption of NOM to the particle surfaces is not fully clear given the qualitative difference between the NOM and extracted humic substances used in many studies (Hitchman et al., 2013; Tejamaya et al., 2012), as no major changes were observed in winter months (where humic substances are likely to be dominant NOM type), the data can be explained without reference to NOM.

3.2.2. Citrate-coated AgNPs

A similar set of experiments to those described above were performed in parallel using citrate-AgNPs. In contrast to the results observed for the PVP-AgNPs exposures, the behaviour of the citrate-AgNPs had more variability between the data for each water condition, which was reflected in the model values.

3.2.3. Spring

Fig. 4A, B and 4C shows the total measured Ag concentration for each of the depths of the microcosm in water collected during spring (April). An average Ag concentration at the top sampling point was significantly higher at 210 ± 135 μg L^{-1} compared to middle and the bottom depths (76 ± 14 μg L^{-1}) between days 1 (24 h) to 28 (672 h). This information shows that the particle dispersion throughout the columns was slow with small Ag losses (Table 2). The modeled particle sizes were 10 nm (comparable to the 'as prepared' citrate-AgNPs of 12 ± 2 nm – Table SI.2). This corresponds to seasonal diffusion coefficients (4.3×10^{-11} $m^2 s^{-1}$), which were inversely proportional to the settling velocities (0.05×10^{-8} m s^{-1}) (Table 2) as observed from the PVP-AgNPs data. After 24 h, the concentration of AgNPs accounted for approximately 98% (2% dissolved) of the total Ag in the surface water and 47% of the total Ag (10% dissolved) in the bottom depth (Table SI.5). When measured on day 28, the AgNP fraction had declined slightly in the surface water accounting for approximately 87%. However, the AgNP concentration in the bottom depth, increased to 67%. Ultrafiltration clearly does not quantify likely changes such as reprecipitation (Tejamaya et al., 2012), although this transformation is likely to occur in this type of water.

TEM data identified small particle size variations from the 'as prepared' AgNPs (28 ± 15 nm at the surface and 46 ± 23 nm at the bottom, after 24 h) (Table SI.6). The results suggest qualitatively that the NPs are less dispersed with some limited aggregation occurring and agrees with the UV–vis findings (Fig. 5C).

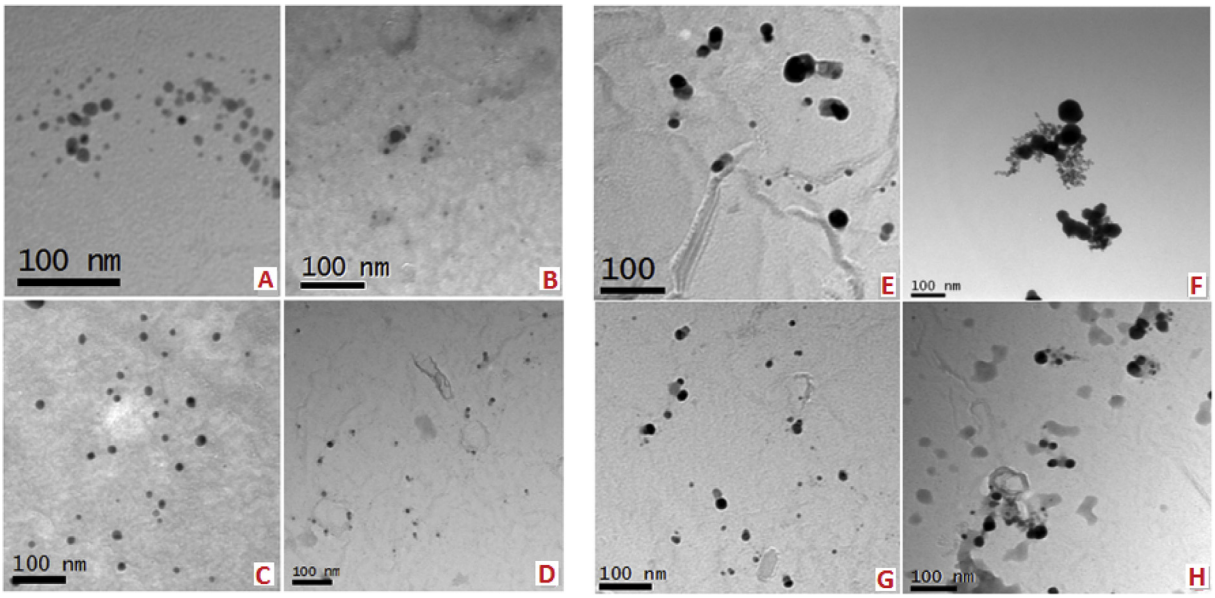

Fig. 3. TEM imaging of the PVP-AgNPs sampled at 24 h from the surface microcosm sampling point of natural water collected during A) spring, B) Summer, C) Autumn and D) Winter seasons. TEM imaging of the citrate AgNPs sampled from E) Spring lake water: 24 h from the surface water, F) Autumn lake water: 24 h from the surface water, G) Spring lake water: 120 h from the surface water and H) Autumn lake water: 120 h from the surface water.

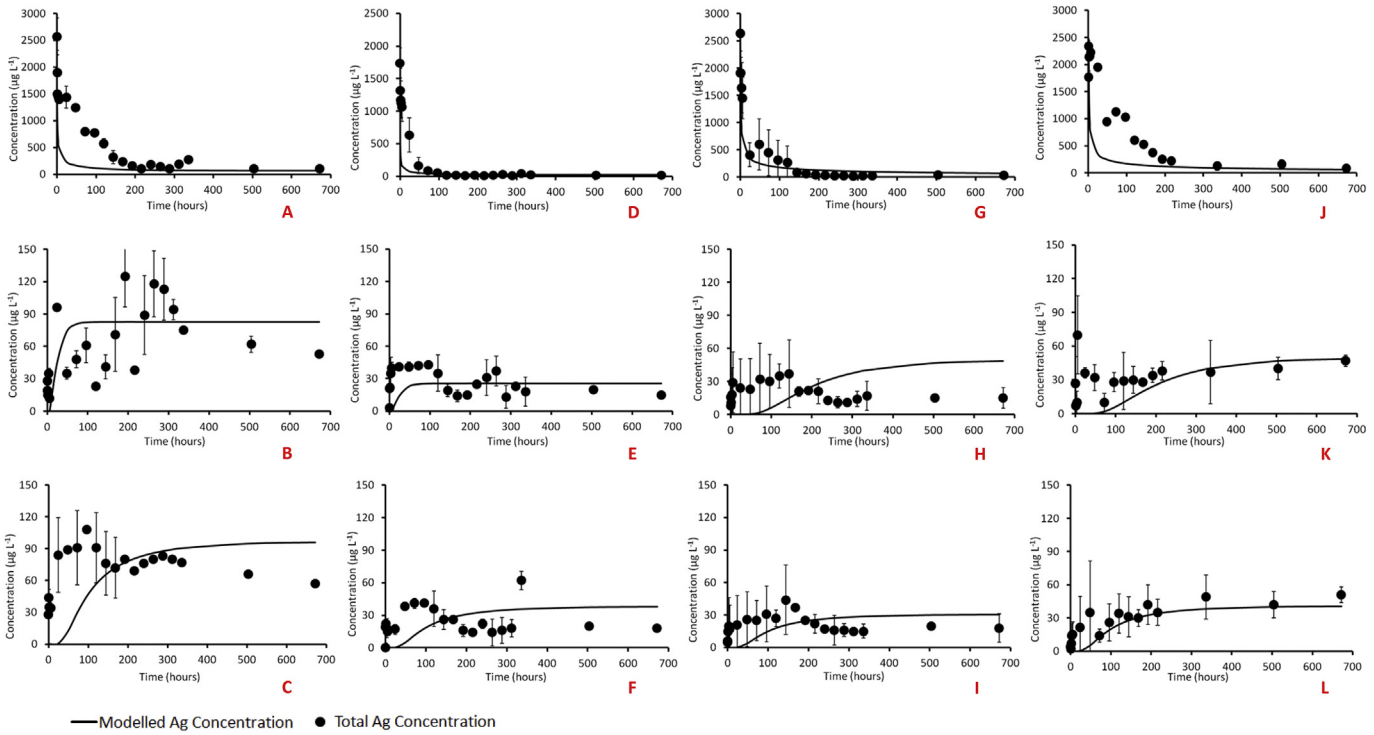

Fig. 4. Observed and modelled total Ag concentrations over time for the citrate-AgNPs study in the surface, middle and bottom depths of the microcosm, in each of the water conditions: A) spring: surface water, B) spring: middle depth water, C) spring: bottom depth water, D) summer: surface water, E) summer: middle depth water, F) summer: bottom depth water, G) autumn: surface water, H) autumn: middle depth water, I) autumn: bottom depth water, J) winter: surface water, K) winter: middle depth water and L) winter: bottom depth water. Dots show the average concentrations of three independent triplicates, error bars represent the standard deviation of the measured concentrations in the three replicated and the solid lines is the fitted model. Mass of Ag NPs introduced to the column fixed at 4.3 mg.

Additionally, the results are generally in agreement with the metal concentration data, and small variants from the modelled results are due to the complexity of the operative processes.

3.2.4. Summer

Citrate-AgNPs observed in the water collected during the summer had concentration losses of up to 70%. Despite these losses, the Ag concentration of 30 ± 26 µg L^{-1} was then consistent over the study period and between each depth, suggesting that there is a moderately persistent fraction of the Ag NPs. In agreement with this, the model residuals (Eq. (5)) were minimized with a M_{Ag} value of 1.6 mg (Fig. 4D, E and 4F; Table 2). Overall, losses of Ag were likely due to sorption or to homo- and hetero-aggregation, followed by sedimentation, with polymer bridging/sorption to larger NOM colloids playing a role in aggregation (Wilkinson et al., 1997; Hinderliter et al., 2010). Furthermore, based on the best fit of the remaining data, the model outputs estimated the sizes of the citrate-AgNPs to be 10 nm, which were comparable within the standard deviation of error to the 'as prepared' citrate-AgNPs of 11 ± 3 nm (Table SI.2). Although it is acknowledged that several complex processes are occurring, AgNPs behaviour is likely to be the same throughout the microcosms. Either there is significant sorption to container walls or larger particles aggregate and sediment to the bottom (Table 1). In both cases, smaller particles remained in suspension where transport was then driven by diffusion and the modeled size is based on the remaining NPs in suspension after losses via aggregation/sedimentation.

The AgNP concentration at 24 h accounted for approximately 98% (2% dissolved) of the total Ag in the surface waters, and 90% (10% dissolved) bottom (Table SI.5). On day 28, the AgNPs (%) fraction in the surface water declined to 54% (46% dissolved) in the surface and 28% (72% dissolved) in the bottom. This information indicates that NOM may have formed incomplete coatings over the available surface areas of the NPs in suspension, or dissociated over time, leading to exposed AgNPs surfaces resulting in dissolution (Hull and Bowman, 2014), and likely to reprecipitation. Studies by Li and Lenhart (2012) and Tejamaya et al. (2012) also reported differences between citrate and PVP coated AgNPs in synthetic waters and concluded that citrate AgNPs were more susceptible to limited aggregation and dissolution (likely followed by reprecipitation) in agreement with our observations.

At 0.5 h, the UV–vis spectra show a slight peak broadening between 500 and 600 nm at 0.5 and 24 h which is absent at later time points (Fig. 5D). This suggests earlier transformations, and would agree with the Ag concentration data showing losses via aggregation and sedimentation. TEM imaging (Fig. 3E, and Figure SI.15) also confirmed small dispersed particles at 24 (13 ± 6 nm) and 72 h (16 ± 8 nm) in the surface water (Table SI.6). Collectively, the information obtained from the UV–vis and the TEM justifies the observations from the model and metal data.

3.2.5. Autumn

The total Ag concentration changes over time in water sampled during the UK autumn season (mid-September) (Fig. 4), show a systematic trend where the Ag concentration increased to a maximum of 37 ± 31 µg L^{-1} at 144 h (day 6) before falling to 11 ± 4 µg L^{-1} at later dates (days 11 and 12) as the AgNPs settled out. Although a number of complex processes occurred, the autumn citrate coated NP behaviour appears to be largely dominated by aggregation and settling. The modelled data gave an NP diameter of 88.4 nm, indicating some aggregation. The M_{Ag} value was 2 mg and the settling velocity 4 × 10^{-8} m s^{-1} (Table 2), indicating that migration of the AgNPs is controlled by sedimentation. Moreover, after 24 h the AgNPs concentration accounted for 100% of the total

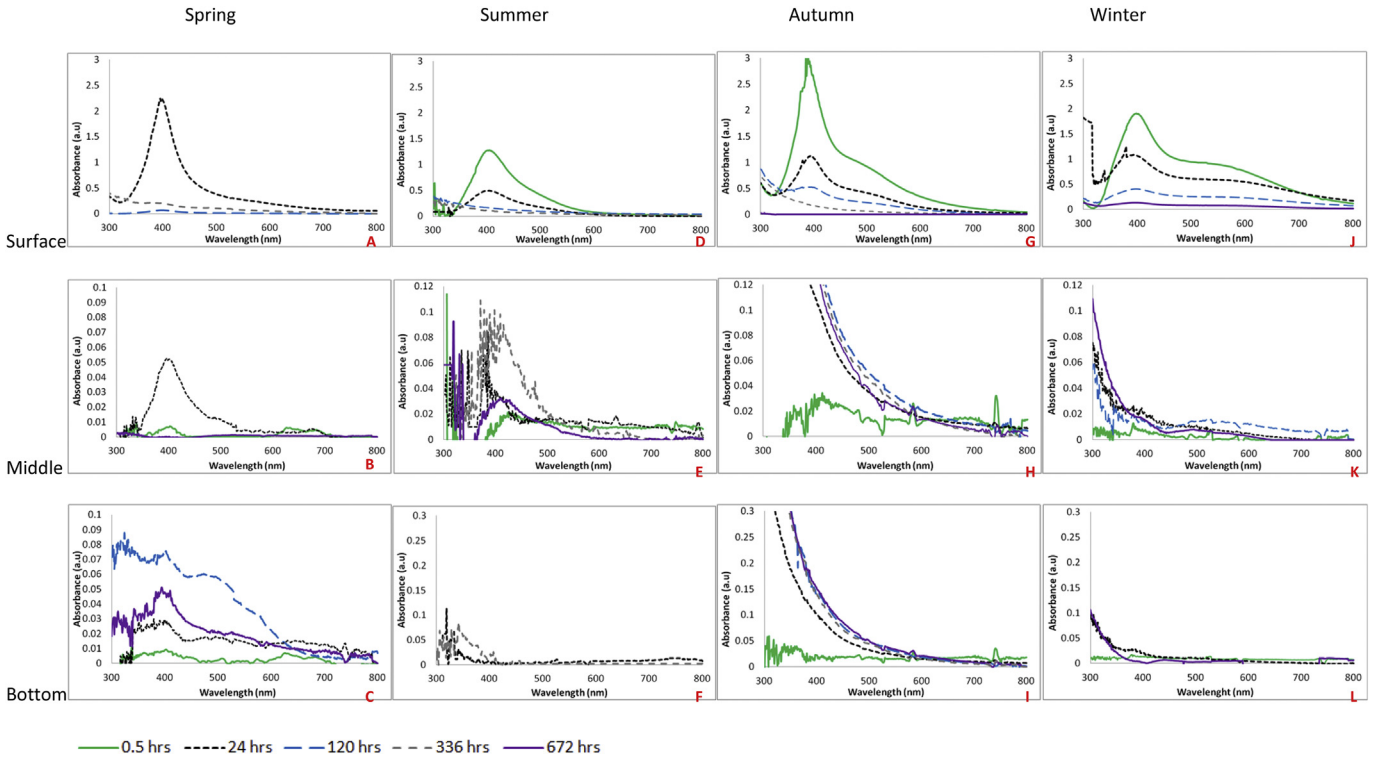

Fig. 5. Comparison SPR profiles of citrate-AgNPs over time for the surface, middle and bottom depths of the microcosm, in each of the water conditions, A) spring: surface water, B) spring: middle depth water, C) spring: bottom depth water, D) summer: surface water, E) summer: middle depth water, F) summer: bottom depth water, G) autumn: surface water, H) autumn: middle depth water, I) autumn: bottom depth water, J) winter: surface water, K) winter: middle depth water and L) winter: bottom depth water.

Ag concentration in the surface waters and 92% in the bottom depths (Table SI.5). Low dissolved concentrations of Ag suggest little dissolution. The reduced dissolution may be ascribed to re-precipitation following dissolution or reduced specific surface area as aggregate sizes increase (Hinderliter et al., 2010).

The UV–vis spectrum for autumn show a bimodal SPR peak at 392 and 500–700 nm (Fig. 5G and H) which was not observed in the 'as prepared UV–vis analysis (Figure SI.2) confirming accelerated aggregation of the citrate-AgNPs (Lodeiro et al., 2016). This is also supported by the rapid loss of SPR peaks in the surface water, with little to no signal in the lower depths (Fig. 5). Due to spectral interferences, it was not possible to view the SPR for the citrate-AgNPs in the middle and bottom depths (Fig. 4H and I) (similar interferences were also observed in the SPR PVP-AgNPs study for the autumn data set).

In agreement with the UV–vis and modelled data, TEM size analysis after 24 h exposure confirmed larger (25 ± 8 nm) AgNPs when compared to the 'as prepared' AgNPs (11 ± 3 nm) in the surface water. Larger AgNPs (60 ± 35 nm; most frequently between 40 and 60 nm in the bottom depth) (Table SI.6) confirmed sedimentation dominated as the larger particles settle. Since this behaviour was not observed for the PVP-AgNPs under the same conditions, the AgNP aggregation behaviour is surface coating specific. Morphological observations in Fig. 3F and SI.10I, SI.10J, SI.10K and SI.10L also confirm aggregated particles (Figure SI.14). Fig. 3F also shows fibrous NOM-like structures that are associated with increased aggregation (Buffle et al., 1998; Wilkinson et al., 1997; Lead et al., 2005), which is comparable with previous microscopy observations of fresh water and from the Vale Lake (investigated in this study) during mid-September (Baalousha et al., 2013). Fulvic and humic acids have previously been documented to adsorb onto the NP surfaces and may increase or decrease stability, depending on conditions (Misra et al., 2012).

Aggregation of the citrate-AgNPs in autumn may be explained by the qualitative difference in the TOC which may include higher concentrations of colloidal organic carbon, polysaccharide and fibrous NOM (time of year dependent), which is much more likely to form sedimenting flocs with NPs resulting in aggregation through the formation of bridges (Wilkinson et al., 1997). Other studies also reported findings of surface interactions between NPs and NOM, which resulted in altered behaviours of the NPs, as observed in our earlier studies (Diegoli et al., 2008; Baalousha, 2009; Baalousha et al., 2013). Therefore, it is highly likely that absorption and bridging flocculation occurred, resulting in the reduced total Ag concentration (Fig. 4G–I) and aggregation of the citrate AgNPs.

3.2.6. Winter

Fig. 4J, K and L show the total measured Ag concentration for water collected during the UK season of winter (January). Between days 5–28, a high concentration of Ag was measured in the surface water of 290 ± 190 μg L^{-1}. To compare, days 5–28 shows the average uniform concentration between the middle and the bottom depths were 33 ± 10 μg L^{-1}, indicating slow Ag concentration dispersion. Similarly to the autumn waters, the modelled concentration (based on the 'as prepared' AgNPs sizes and starting concentrations) did not match the measured Ag concentrations. The model estimated Ag mass (M_{Ag}) of 2 mg (Table 2), reflecting Ag losses either by sedimentation or sorption on the microcosm walls. High Ag concentrations in the lower depths at earlier time points (Fig. 4K and L, between 0 and 24 h) suggest that AgNPs behaviour is dominated by aggregation and sedimentation. This is further supported by the increase in AgNPs sedimentation velocity (Table 2).

When sampled at 24 h, the total Ag concentration in the surface water accounted for 100% AgNPs compared to 70% AgNPs (30% dissolved) at the bottom depth (Table SI.5). After 28 days, the AgNP

concentration accounted for 98% of the total Ag in the surface waters and 88% in the bottom depths (Table SI.6). The increased AgNPs concentration over time, observed in this study was most likely due to reprecipitation of dissolved Ag and limited dissolution of this new material (Hinderliter et al., 2010; Hull and Bowman, 2014).

The UV–vis profiles (Fig. 5J, K and L) identified a bimodal SPR peak at 392 and 500–700 nm at all time points recorded, confirming rapid aggregation of the citrate-AgNPs (Lodeiro et al., 2016). Additionally, after 24 h TEM size analysis identified larger AgNPs in the surface (Table SI.6: 16 ± 5 nm) and bottom (19 ± 7 nm) when compared to the 'as prepared' AgNPs (Table SI.2: 12 ± 2 nm). Furthermore, the AgNPs sizes increased to 225 ± 173 nm in the bottom depth after 5 days (120 h). No size observations for the surface water were made, due to low concentrations of particles required for statistical significance (100 particles). Morphological observations (Figure SI.10M, SI.10N, SI.10O and SI.10P) show larger and aggregated particles at 24 h (day 1) and 120 h (day 5), improving the reliability of the model and UV–vis results to confirm size increases. EDS (Figure SI.15) confirmed the particles observed were Ag.

4. Conclusions

This study used different surface coated AgNPs (citrate and PVP) to address their fate and behaviour in seasonally different natural lake waters in microcosm columns. AgNPs fate and behaviour as interpreted through aggregation, sedimentation and dissolution was dependent on NP properties and solution conditions. For the citrate coated NPs, a variety of different behaviors were observed and inferred. In addition to dissolution, aggregation and sedimentation, reprecipitation and sorption to container walls are thought to be important. The citrate-AgNPs behaviour was dominated by the seasonal changes in solution chemistry and PVP-AgNPs were largely unaffected with limited transformations occurred.

Acknowledgments

We thank the Natural Environment Research Council (NERC) NanoBEE consortium (NE/H013148/1) for their financial support. We also acknowledge the support of the NERC funded Facility for Environmental Nanoscience Analysis and Characterization (FENAC). The SmartState Center for Environmental Nanoscience and Risk is also thanked for financial support.

Appendix A. Supplementary data

Supplementary data related to this article can be found at https://doi.org/10.1016/j.chemosphere.2017.10.006.

References

Afshinnia, K., Sikder, M., Cai, B., Baalousha, M., 2017. Effect of nanomaterial and media physicochemical properties on Ag NM aggregation kinetics. J. Colloid Interface Sci. 487, 192–200.
Asghari, S., Johari, S.A., Lee, J.H., Kim, Y.S., Jeon, Y.B., Choi, H.J., Moon, M.C., Yu, I.J., 2012. Toxicity of various silver nanoparticles compared to silver ions in Daphnia magna. J. Nanobiotechnol. 10, 1.
Baalousha, M., 2009. Aggregation and disaggregation of iron oxide nanoparticles: influence of particle concentration, pH and natural organic matter. Sci. Total Environ. 407, 2093–2101.
Baalousha, M., Arkill, K., Romer, I., Palmer, R., Lead, J., 2015. Transformations of citrate and Tween coated silver nanoparticles reacted with Na 2 S. Sci. Total Environ. 502, 344–353.
Baalousha, M., Nur, Y., Römer, I., Tejamaya, M., Lead, J., 2013. Effect of monovalent and divalent cations, anions and fulvic acid on aggregation of citrate-coated silver nanoparticles. Sci. Total Environ. 454, 119–131.
Bae, S., Hwang, Y.S., Lee, Y.-J., Lee, S.-K., 2013. Effects of water chemistry on aggregation and soil adsorption of silver nanoparticles. Environ. health Toxicol. 28.
Benn, T.M., Westerhoff, P., 2008. Nanoparticle silver released into water from commercially available sock fabrics. Environ. Sci. Technol. 42, 4133–4139.
Buffle, J., Wilkinson, K.J., Stoll, S., Filella, M., Zhang, J., 1998. A generalized description of aquatic colloidal interactions: the three-colloidal component approach. Environ. Sci. Technol. 32, 2887–2899.
Chen, K.L., Elimelech, M., 2007. Influence of humic acid on the aggregation kinetics of fullerene (C 60) nanoparticles in monovalent and divalent electrolyte solutions. J. Colloid Interface Sci. 309, 126–134.
Chinnapongse, S.L., Maccuspie, R.I., Hackley, V.A., 2011. Persistence of singly dispersed silver nanoparticles in natural freshwaters, synthetic seawater, and simulated estuarine waters. Sci. total Environ. 409, 2443–2450.
Cumberland, S.A., Lead, J.R., 2009. Particle size distributions of silver nanoparticles at environmentally relevant conditions. J. Chromatogr. A 1216, 9099–9105.
Diegoli, S., Manciulea, A.L., Begum, S., Jones, I.P., Lead, J.R., Preece, J.A., 2008. Interaction between manufactured gold nanoparticles and naturally occurring organic macromolecules. Sci. Total Environ. 402, 51–61.
Doucet, F.J., Maguire, L., Lead, J.R., 2004. Size fractionation of aquatic colloids and particles by cross-flow filtration: analysis by scanning electron and atomic force microscopy. Anal. Chim. Acta 522, 59–71.
Ellis, L.-J.A., Valsami-Jones, E., Lead, J.R., Baalousha, M., 2016. Impact of surface coating and environmental conditions on the fate and transport of silver nanoparticles in the aquatic environment. Sci. Total Environ. 568, 95–106.
EPA, U.S.E.P.A.U., 2009. Method 415.3: Determination of Total Organic Carbon and Specific UV Absorbance at 254 Nm in Source Water and Drinking Water. Revision 1.2. Ed.
Fabrega, J., Luoma, S.N., Tyler, C.R., Galloway, T.S., Lead, J.R., 2011a. Silver nanoparticles: behaviour and effects in the aquatic environment. Environ. Int. 37, 517–531.
Fabrega, J., Zhang, R., Renshaw, J.C., Liu, W.-T., Lead, J.R., 2011b. Impact of silver nanoparticles on natural marine biofilm bacteria. Chemosphere 85, 961–966.
Gottschalk, F., Sun, T., Nowack, B., 2013. Environmental concentrations of engineered nanomaterials: review of modeling and analytical studies. Environ. Pollut. 181, 287–300.
Hendren, C.O., Mesnard, X., Dröge, J., Wiesner, M.R., 2011. Estimating production data for five engineered nanomaterials as a basis for exposure assessment. Environ. Sci. Technol. 45, 2562–2569.
Hendricks, D.W., 2006. Water Treatment Unit Processes: Physical and Chemical. CRC press.
Hinderliter, P.M., Minard, K.R., Orr, G., Chrisler, W.B., Thrall, B.D., Pounds, J.G., Teeguarden, J.G., 2010. ISDD: a computational model of particle sedimentation, diffusion and target cell dosimetry for in vitro toxicity studies. Part. fibre Toxicol. 7, 36.
Hitchman, A., Smith, G.H.S., Ju-Nam, Y., Sterling, M., Lead, J.R., 2013. The effect of environmentally relevant conditions on PVP stabilised gold nanoparticles. Chemosphere 90, 410–416.
Hull, M., Bowman, D., 2014. Nanotechnology Environmental Health and Safety: Risks, Regulation, and Management. William Andrew.
Huynh, K.A., Chen, K.L., 2011. Aggregation kinetics of citrate and polyvinylpyrrolidone coated silver nanoparticles in monovalent and divalent electrolyte solutions. Environ. Sci. Technol. 45, 5564–5571.
Ju-Nam, Y., Lead, J.R., 2008. Manufactured nanoparticles: an overview of their chemistry, interactions and potential environmental implications. Sci. total Environ. 400, 396–414.
Kennedy, A.J., Hull, M.S., Bednar, A.J., Goss, J.D., Gunter, J.C., Bouldin, J.L., Vikesland, P.J., Steevens, J.A., 2010. Fractionating nanosilver: importance for determining toxicity to aquatic test organisms. Environ. Sci. Technol. 44, 9571–9577.
King, S.M., Jarvie, H.P., Bowes, M.J., Gozzard, E., Lawlor, A.J., Lawrence, M.J., 2015. Exploring controls on the fate of PVP-capped silver nanoparticles in primary wastewater treatment. Environ. Sci. Nano 2, 177–190.
Kvitek, L., PanácEK, A., Soukupova, J., Kolar, M., Vecerova, R., Prucek, R., Holecová, M., Zboril, R., 2008. Effect of surfactants and polymers on stability and antibacterial activity of silver nanoparticles (NPs). J. Phys. Chem. C 112, 5825–5834.
Lead, J., Muirhead, D., Gibson, C., 2005. Characterization of freshwater natural aquatic colloids by atomic force microscopy (AFM). Environ. Sci. Technol. 39, 6930–6936.
Lodeiro, P., Achterberg, E.P., Pampín, J., Affatati, A., El-Shahawi, M.S., 2016. Silver nanoparticles coated with natural polysaccharides as models to study AgNP aggregation kinetics using UV-Visible spectrophotometry upon discharge in complex environments. Sci. Total Environ. 539, 7–16.
Li, X., Lenhart, J.J., 2012 Apr 25. Aggregation and dissolution of silver nanoparticles in natural surface water. Environ. Sci. Technol. 46 (10), 5378–5386.
Lowry, G.V., Gregory, K.B., Apte, S.C., Lead, J.R., 2012. Transformations of nanomaterials in the environment. Environ. Sci. Technol. 46, 6893–6899.
Misra, S.K., Dybowska, A., Berhanu, D., Luoma, S.N., Valsami-Jones, E., 2012. The complexity of nanoparticle dissolution and its importance in nanotoxicological studies. Sci. Total Environ. 438, 225–232.
Mueller, N.C., Nowack, B., 2008. Exposure modeling of engineered nanoparticles in the environment. Environ. Sci. Technol. 42, 4447–4453.
Nowack, B., Baalousha, M., Bornhöft, N., Chaudhry, Q., Cornelis, G., Cotterill, J., Gondikas, A., Hassellöv, M., Lead, J., Mitrano, D.M., 2015. Progress towards the validation of modeled environmental concentrations of engineered nanomaterials by analytical measurements. Environ. Sci. Nano 2, 421–428.

Nowack, B., Ranville, J.F., Diamond, S., Gallego-Urrea, J.A., Metcalfe, C., Rose, J., Horne, N., Koelmans, A.A., Klaine, S.J., 2012. Potential scenarios for nanomaterial release and subsequent alteration in the environment. Environ. Toxicol. Chem. 31, 50–59.

Piccapietra, F., Sigg, L., Behra, R., 2011. Colloidal stability of carbonate-coated silver nanoparticles in synthetic and natural freshwater. Environ. Sci. Technol. 46, 818–825.

Pokhrel, L.R., Dubey, B., Scheuerman, P.R., 2014. Natural water chemistry (dissolved organic carbon, pH, and hardness) modulates colloidal stability, dissolution, and antimicrobial activity of citrate functionalized silver nanoparticles. Environ. Sci. Nano 1, 45–54.

Roh, J., Umh, H.N., Sim, J., Park, S., Yi, J., Kim, Y., 2013. Dispersion stability of citrate- and PVP-AgNPs in biological media for cytotoxicity test. Korean J. Chem. Eng. 30, 671–674.

Sharma, V.K., Siskova, K.M., Zboril, R., Gardea-Torresdey, J.L., 2014. Organic-coated silver nanoparticles in biological and environmental conditions: fate, stability and toxicity. Adv. Colloid Interface Sci. 204, 15–34.

Socolofsky, S.A., Jirka, G.H., 2005. Special Topics in Mixing and Transport Processes in the Environment, fifth ed. Coastal and Ocean Engineering Division, Texas A&M University. Engineering—lectures.

Sun, T.Y., Bornhöft, N.A., Hungerbühler, K., Nowack, B., 2016. Dynamic probabilistic modeling of environmental emissions of engineered nanomaterials. Environ. Sci. Technol. 50, 4701–4711.

Tejamaya, M., Römer, I., Merrifield, R.C., Lead, J.R., 2012. Stability of citrate, PVP, and PEG coated silver nanoparticles in ecotoxicology media. Environ. Sci. Technol. 46, 7011–7017.

Wilkinson, K.J., Negre, J.-C., Buffle, J., 1997. Coagulation of colloidal material in surface waters: the role of natural organic matter. J. Contam. Hydrology 26, 229–243.